

Tailoring PTV expansion to improve the dosimetry of post modified radical mastectomy intensity-modulated radiotherapy for left-sided breast cancer patients by using 4D CT combined with cone beam CT

Jiyong Zhang¹ | Lei Huang¹ | Fangcai Wu¹ | Guoxi Wang¹ | Lili Wu¹ |
Baotian Huang¹ | Yan Lin² | Dongsheng Li¹ | Changchun Ma^{1,3}

¹Department of Radiation Oncology, Cancer Hospital of Shantou University Medical College, Shantou, China

²Department of Medical Imaging, The Second Affiliated Hospital, Shantou University Medical College, Shantou, China

³Guangdong Provincial Key Laboratory for Breast Cancer Diagnosis and Treatment, Cancer Hospital of Shantou University Medical College, Shantou, China

Author to whom correspondence should be addressed. Changchun Ma
E-mail: 994370958@qq.com; Telephone: 86-13829633639; Fax: 86-0754-88560352.

Funding information

Natural Science Foundation of Guangdong Province, Grant/Award Number: 2018A030307050; National Natural Science Foundation of China, Grant/Award Number: 82071973; Medical Scientific Research Foundation of Guangdong Province, Grant/Award Number: B2017025; Guangdong Provincial Key Laboratory for Breast Cancer Diagnosis and Treatment(2017B030314116).

Abstract

Purpose: Our study aimed to improve the dosimetry of post modified radical mastectomy intensity-modulated radiotherapy (PMRM-IMRT) for left-sided breast cancer patients by tailoring and minimizing PTV expansion three-dimensionally utilizing 4D CT combined with on-board cone beam CT (CBCT).

Methods: We enrolled a total of 10 consecutive left-sided breast cancer patients to undergo PMRM-IMRT. We measured the intra-fractional CTV displacement attributed to respiratory movement by defining 9 points on the left chest wall and quantifying their displacement by using the 4D CT, and measured the inter-fractional CTV displacement resulting from the integrated effect of respiratory movement, thoracic deformation and set up errors by using CBCT. We created 3 different PMRM-IMRT plans for each of the patients using PTV_t (tailored PTV expansion three-dimensionally), PTV_{0.5} and PTV_{0.7} (isotropic 0.5- cm and isotropic 0.7- cm expanding margin of CTV), respectively. We performed paired samples t test to establish a hierarchy in terms of plan quality and dosimetric benefits. $P < 0.05$ was considered statistically significant.

Results: The inter-fractional CTV displacement (2.6 ± 2.2 mm vertically, 2.8 ± 2.3 mm longitudinally, and 1.7 ± 1.2 mm laterally) measured by CBCT was much larger than the intra-fractional one (0.5 ± 0.5 mm vertically, 0.5 ± 1.0 mm longitudinally, and 0.3 ± 0.3 mm laterally, respectively) measured by 4D CT. Intensity-modulated radiotherapy with tailored PTV expansion based on inter-fractional CTV displacement had dosimetric advantages over those with PTV_{0.5} or those with PTV_{0.7} owing to its perfect PTV dose coverage and better OARs sparing (especially of heart and left lung).

Abbreviations: PTV, plan target volume; 4D CT, four-dimensional computed tomography; PMRM-IMRT, post modified radical mastectomy intensity-modulated radiotherapy; CT, cone beam CT; CTV, clinical target volume; OAR, organ at risk

*Changchun Ma and Dongsheng Li jointly supervised this work.

†Jiyong Zhang and Lei Huang contributed equally to this work.

This is an open access article under the terms of the Creative Commons Attribution License, which permits use, distribution and reproduction in any medium, provided the original work is properly cited.

© 2021 The Authors. *Journal of Applied Clinical Medical Physics* published by Wiley Periodicals, Inc. on behalf of American Association of Physicists in Medicine.

Conclusion: The CTV displacement in PMRM-IMRT predominantly arises from inter-fraction rather than from intra-fraction during natural respiration and differs in 3 coordinate axes either inter-fractionally or intra-fractionally. Tailoring and minimizing PTV expansion three-dimensionally significantly improves the dosimetry of PMRM-IMRT for left-sided breast cancer patients.

KEY WORDS

dosimetry, intra-fractional CTV displacement, inter-fractional CTV displacement, intensity-modulated radiotherapy, left-sided breast cancer, post modified radical mastectomy, tailoring PTV expansion

1 | INTRODUCTION

Our previous study had demonstrated that intensity-modulated radiation therapy has dosimetrical advantages over three-dimensional conformal radiotherapy with field-in-field technique (3DCRT-FinF) and 2-partial arc volumetric modulated arc therapy (2P-VMAT) for left-sided breast cancer patients after modified radical mastectomy, and suggested that individually quantifying and minimizing CTV displacement might improve target dose coverage and heart and left lung sparing.¹ Given the heart irradiation leading to the subsequent increasing risk of life-threatening major cardiac events, including myocardial infarction, coronary revascularization, or death from ischemic cardiac disease,²⁻⁷ and the nature of lack of a threshold value, their long-term, dosage-related effect as well as the additive nature of the risk with preexisting cardiac diseases,⁸ heart radiation exposure should be used as an a priori limitation parameter to evaluate which of the radiotherapy plans for left-sided breast cancer after modified radical mastectomy is more advantageous if PTV dose coverage and other OARs sparing are acceptable.¹ Our study aimed to verify the dosimetry improvement of post modified radical mastectomy intensity-modulated radiotherapy (PMRM-IMRT) for the patients by tailoring and minimizing PTV expansion three-dimensionally utilizing four-dimensional computed tomography (4D CT) simulation combined with on-board cone beam CT (CBCT) verification under natural respiration.

2 | MATERIALS AND METHODS

We enrolled a total of 10 left-sided breast cancer patients undergoing IMRT after modified radical mastectomy in this study. Based on the contouring atlas published by the Radiation Therapy Oncology Group (RTOG),⁹ we delineated CTV including left chest wall and ipsilateral lymph node drainage area. A prescribed dose of 50 Gy/5w/25f was delivered to PTV. Each patient had 4D CT simulation before radiotherapy and three times of on-board cone beam CT verification inter-fractionally during the treatment. The intra-fractional CTV displacement attributed to respiratory movement was measured by the 4D CT. The inter-fractional CTV displacement resulting from the integrated effect of respiratory movement, thoracic disformation and setup errors was measured by the on-board cone beam CT.

The study was performed in accordance with the Declaration of Helsinki, and was approved by the Ethics Committee of the Cancer Hospital of Shantou University Medical College. Informed consent form was obtained from each patient.

2.A | 4D CT simulation

Each patient was placed in a supine position. Three lateral lines (labeled with 1, 2, and 3) were marked on the surface of the left chest wall using laser projecting across the lower edge of bilateral sternal heads, right nipple and the skinfold of the lower edge of the right breast, respectively. The other three longitudinal lines (named A, B, and C) were labeled across the left edge of the sternum, left mid-clavicular line and left anterior axillary, respectively. The intersection points (A1, A2, A3, B1, B2, B3, C1, C2, and C3) of the three lateral and the three longitudinal lines were marked with ink and radiopaque metal beads on the surface of the left chest wall. The position changes of A1, A2, A3, B1, B2, B3, C1, C2, and C3 points measured by 4D CT were documented to reflect the intra-fractional CTV displacement attributed to respiratory movement. For each patient, a helical CT scan was acquired under natural breathing followed by 4D CT scans taken at a representative normal respiratory cycle using a Philips Brilliance CT Big Bore Simulation System (Andover, MA). The respiratory signal was recorded with the Real-Time Position Management (RPM) Respiratory Gating System (Varian Medical System, Palo Alto, CA) and synchronized with the CT data. The slice thickness was 3 mm at 512 × 512 pixels. Each image acquired and tagged to its corresponding phase of the respiratory cycle was then sent to the workstation using the 4D CT software. The position changes of A1, A2, A3, B1, B2, B3, C1, C2, and C3 points were documented to reflect the intra-fractional CTV displacement attributed to respiratory movement. X, Y, and Z values indicated the displacement of the intersection points in x (laterally), in y (longitudinally) and in z coordinate axis (vertically), respectively.

2.B | 3D on-board cone beam CT verification

Each patient had a total of three times of on-board cone beam CT verification inter-fractionally randomly during the treatment.

The CBCT scans were performed using the on-board imager system installed on the Varian TrueBeam linac (Varian Medical System, Palo Alto, CA, USA). Under the half-fan scan mode (field of view = 46 cm), the detector is centered laterally and longitudinally with respect to the source. The CBCT protocols used 1080 mAs at 125 kV with weighted CT dose index (CTDI_w) of 1.60 Gy. The CBCT image acquired in half-fan mode and reconstructed using manufacturer's software. Patient position shifts in x, y, and z directions were documented after manually matching the radiopaque markers (the sternum and the labeled metal beads on the chest wall) between their initial simulation position and the present on-board position.

2.C | Plan comparison and statistical analysis

We created three different PMRM-IMRT plans for each of the patients using the PTV_t (tailored PTV expansion three-dimensionally), PTV_{0.5} and PTV_{0.7} (isotropic 0.5-cm and isotropic 0.7-cm expanding margin of CTV), respectively. All PMRM-IMRT plans used two opposed tangential beams, and two anterior beams with a 10-degree angle from the tangential ones, and a supraclavicular beam. The dose calculations were employed with a grid of 2.5 mm using the Anisotropic Analytical Algorithm (AAA). All plans were created with a prescribed dose of 50 Gy covering 95% of the PTV.

Clinical target volume (CTV) and OARs including heart, ipsilateral lung, spinal cord, and contralateral breast were contoured as previously¹ using the Eclipse treatment planning system (Eclipse 10.0, Varian Medical Systems, Palo Alto, CA, USA). D_{mean}, V_{95%}, V_{105%}, heterogeneity index (HI) and conformity index (CI) values were calculated for the PTV. V_{95%} was defined as the percentage of the PTV receiving 95% or more of the prescription dose. V_{105%} indicated the dose hotspot area that received 105% of the prescription dose. The heterogeneity index (HI) and conformity index (CI) were calculated as followed: $HI = (D_{2\%} - D_{98\%}) / D_{50\%}$, $CI = (V_{PTVref} / V_{PTV}) \times (V_{PTVref} / V_{ref})$, where V_{PTVref} represents the volume of PTV covered with the reference dose. V_{PTV} represents the volume of PTV and V_{ref} represents the volume covered with the reference dose or higher. A lower HI value, ranging from 0 to 1, represents better homogeneity. A lower CI value, ranging from 0 to 1, represents worse conformity. D_{mean} is an average dose delivering to an organ. V_(xGy) represents the percentage of an organ's volume receiving (x) Gy or higher. D_{2%} represented the dose corresponding to 2% PTV volume as shown in the dose volume histogram (DVH) and could be deemed as the maximum dose, whereas D_{98%} could be deemed as the minimum dose. D_{50%} represented the reference dose (or prescription dose) for PTV. D_{mean}, V_{5 Gy}, V_{10 Gy}, and V_{20 Gy} were calculated for the heart and the left lung. We performed paired samples t test between any two of the three plans, to establish a hierarchy in terms of plan quality and dosimetric benefits. P < 0.05 were considered statistically significant. The SPSS 19.0 software (IBM, Chicago, IL) was used for statistical data management and analysis. P < 0.05 was considered statistically significant.

3 | RESULTS

The intra-fractional CTV displacement in PMRM-IMRT for left-sided breast cancer patients measured by 4D CT during natural respiration.

The overall intra-fractional CTV displacement attributed to respiratory movement measured by 4D CT simulation differed in three directions, with 0.5 ± 0.5 mm vertically, 0.5 ± 1.0 mm longitudinally, and 0.3 ± 0.3 mm laterally, respectively. As exhibited in Table 1, the result indicated that the lower and lateral part of the chest wall tends to have a larger range of displacement than the upper and middle one during natural breathing. Either the displacement in y direction or in z direction was larger than in x direction during natural respiration (Table 1).

The inter-fractional CTV displacement in PMRM-IMRT for left-sided breast cancer patients measured by CBCT during natural breathing.

The inter-fractional CTV displacement in PMRM-IMRT was much larger than the intra-fractional one during natural breathing. The inter-fractional CTV displacement resulting from the mixed effect of respiratory movement, thoracic disformation and setup errors, measured by on-board cone beam CT were 2.6 ± 2.2 mm vertically, 2.8 ± 2.3 mm longitudinally, and 1.7 ± 1.2 mm laterally, respectively (Table 2). The CTV displacement predominantly arises from inter-fraction rather than from intra-fraction during natural breathing, and differs in three directions either inter-fractionally or intra-fractionally.

Dosimetrical advantage of PMRM-IMRT using PTV_t over those using PTV_{0.5} or those using PTV_{0.7} for left-sided breast cancer patients under natural respiration.

TABLE 1 The intra-fractional CTV displacement in PMRM-IMRT for left-sided breast cancer measured by 4D CT.

Parameters	X (mm)	Y (mm)	Z (mm)
A1	0.2 ± 0.2	0.4 ± 0.1	0.4 ± 0.4
A2	0.3 ± 0.3	0.5 ± 0.1	0.5 ± 0.4
A3	0.3 ± 0.3	0.4 ± 0.8	0.7 ± 0.5
B1	0.2 ± 0.4	0.5 ± 0.1	0.6 ± 0.6
B2	0.4 ± 0.4	0.5 ± 1.0	0.6 ± 0.6
B3	0.4 ± 0.4	0.5 ± 1.0	0.6 ± 0.5
C1	0.2 ± 0.3	0.6 ± 1.1	0.7 ± 0.7
C2	0.5 ± 0.4	0.5 ± 1.0	0.3 ± 0.3
C3	0.4 ± 0.3	0.5 ± 0.9	0.5 ± 0.4

The intersection points (A1, A2, A3, B1, B2, B3, C1, C2, and C3) of the three lateral and the three longitudinal lines were marked with ink and radiopaque metal beads on the surface of the left chest wall. The displacement of the intersection points was measured to quantify the position change of the left-sided chest wall. X, Y, and Z values indicated the displacement of the intersection points in x (laterally), in y (longitudinally), and in z coordinate axis (vertically), respectively. Data presented as mean ± standard deviation (mm). Abbreviations: PMRM-IMRT = post modified radical mastectomy intensity-modulated radiotherapy. 4D CT = four-dimensional computed tomography.

TABLE 2 Much larger inter-fractional CTV displacement measured by CBCT than the intra-fractional one in PMRM-IMRT for left-sided breast cancer during peaceful breathing.

Parameters	Direction	Number	Mean \pm SD(mm)	≤ 2 mm	≤ 3 mm	≤ 4 mm
Intra-fraction	X	900	0.3 \pm 0.3	99.7%	100.0%	100.0%
	Y	900	0.5 \pm 1.0	88.1%	96.5%	100.0%
	Z	900	0.5 \pm 0.5	96.5%	99.5%	100.0%
	Sum	2700	0.4 \pm 0.7	94.8%	98.7%	100.0%
Inter-fraction	X	30	1.7 \pm 1.2	40.0%	93.3%	96.6%
	Y	30	2.8 \pm 2.3	46.6%	60.0%	63.3%
	Z	30	2.6 \pm 2.2	50.0%	66.6%	70.0%
	Sum	90	2.4 \pm 2.1	45.5%	73.3%	76.6%

X, Y, and Z values indicated the inter- or intra-fractional CTV displacement in x (laterally), in y (longitudinally) and in z coordinate axis (vertically), respectively. Data presented as mean \pm standard deviation (Mean \pm SD) (mm). The values in the last three columns were the CTV coverage rates under the corresponding status when using CTV expanding values with 2, 3, and 4 mm, respectively. Abbreviations: PMRM-IMRT = post modified radical mastectomy intensity-modulated radiotherapy. CBCT = cone beam computed tomography.

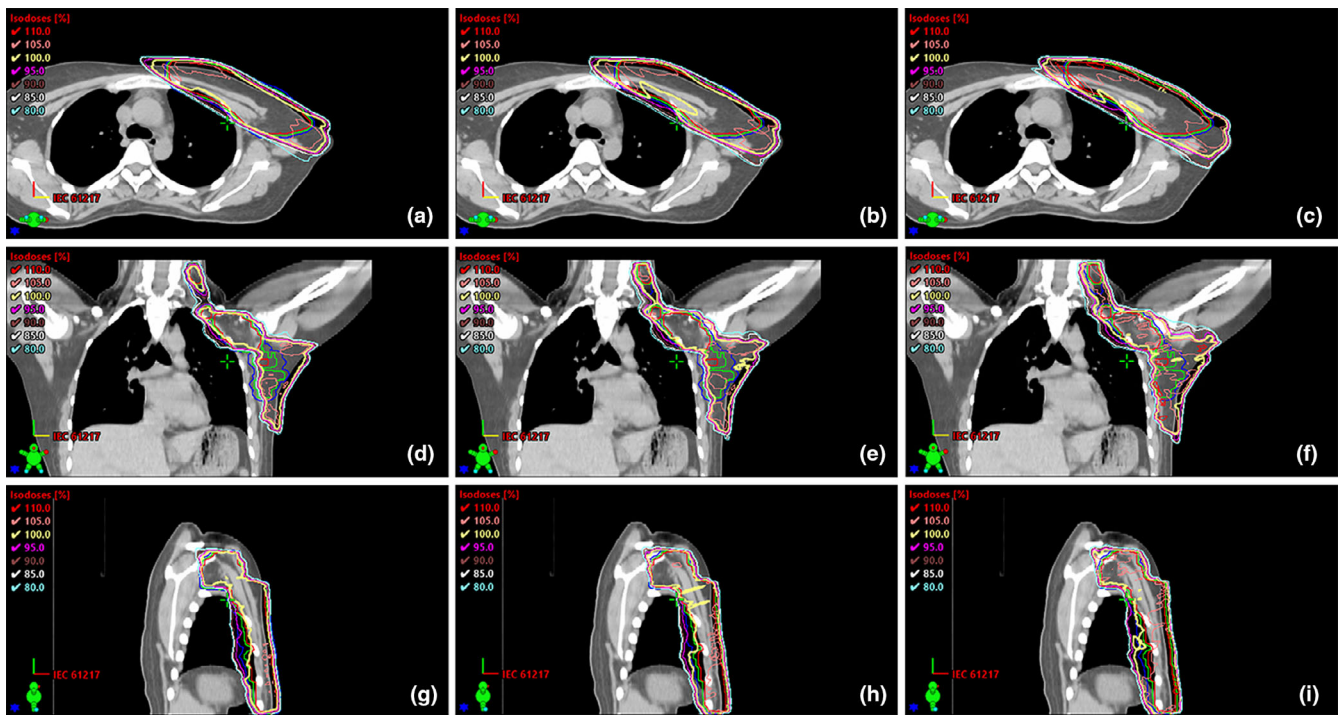


FIG. 1. Transverse, coronal and sagittal dose distribution curves for the three PMRM-IMRT plans using PTV_t (red), $PTV_{0.5}$ (green), and $PTV_{0.7}$ (blue) in a representative patient. (a, b, c), (d, e, f), and (g, h, i) exhibited dosage distribution in the transverse section, the coronal plane and the sagittal plane. PTV_t (red), $PTV_{0.5}$ (green) and $PTV_{0.7}$ (blue) were used to represent the three PMRM-IMRT plans, respectively.

We expanded CTV 3 mm in x, 4 mm in y, and 4 mm in z direction (the average value of the inter-fractional CTV displacement without correction or optimization) to generate PTV_t and created the corresponding IMRT plans. We have performed Shapiro-Wilk test for each group of the raw data (including D_{mean} , $D_{2\%}$, $D_{50\%}$, $D_{98\%}$, $V_{95\%}$, $V_{105\%}$, CI and HI of PTV , D_{mean} , V_5 Gy, V_{10} Gy, and V_{20} Gy of Heart, D_{mean} , V_5 Gy, V_{10} Gy, and V_{20} Gy of Left Lung, D_{mean} of Right Breast, D_{max} of Spinal Cord) and found that they are of the Gaussian distribution. The PMRM-IMRT using PTV_t ($V_{95\%} = 99.57 \pm 0.20$, HI = 0.085 \pm 0.01) provided perfect PTV dose coverage and the best homogeneity compared with those using

$PTV_{0.5}$ ($V_{95\%} = 99.30 \pm 0.55$, HI = 0.095 \pm 0.01) or those using $PTV_{0.7}$ ($V_{95\%} = 99.04 \pm 0.29$, HI = 0.117 \pm 0.01). Moreover, the OARs including heart, left lung, right breast, spinal cord, healthy tissue in PMRM-IMRT using PTV_t (heart- $D_{mean} = 9.01 \pm 2.67$ Gy, left lung- $D_{mean} = 14.47 \pm 1.15$ Gy, right breast- $D_{mean} = 3.09 \pm 2.24$ Gy, spinal cord - $D_{max} = 5.76 \pm 2.99$ Gy, healthy tissue- $D_{mean} = 7.87 \pm 1.19$ Gy) had significantly lower radiation exposure compared with those using $PTV_{0.5}$ (heart- $D_{mean} = 9.84 \pm 2.67$ Gy, left lung- $D_{mean} = 15.45 \pm 0.95$ Gy, right breast- $D_{mean} = 3.57 \pm 2.46$ Gy, spinal cord - $D_{max} = 8.12 \pm 3.48$ Gy, healthy tissue- $D_{mean} = 8.48 \pm 1.18$ Gy) (all $P < 0.01$) or those using $PTV_{0.7}$ (heart- $D_{mean} = 11.10 \pm 2.97$ Gy, left

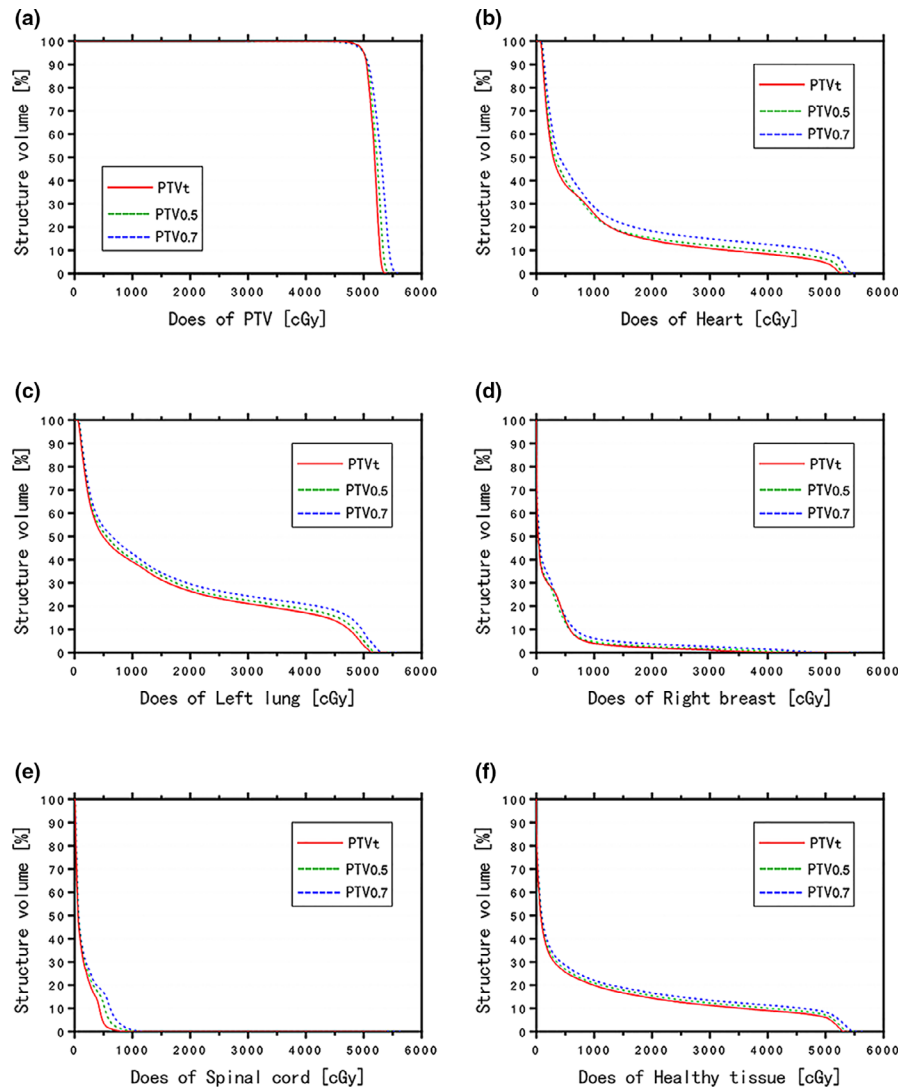


FIG. 2. Comparison of dose volume histograms (DVHs) among the three PMRM-IMRT plans using PTV_t (red), PTV_{0.5} (green), and PTV_{0.7} (blue), respectively. The charts showed the DVHs for PTV (a), heart (b), left lung (c), right breast (d), spinal cord (e) and healthy tissue (f).

lung- $D_{\text{mean}} = 16.53 \pm 1.22$ Gy, right breast- $D_{\text{mean}} = 4.12 \pm 2.85$ Gy, spinal cord- $D_{\text{max}} = 9.76 \pm 3.23$ Gy, healthy tissue- $D_{\text{mean}} = 9.06 \pm 1.19$ Gy) (all $P < 0.05$). Additionally, PMRM-IMRT plans using PTV_{0.5} also had satisfactory PTV dose coverage and better OARs including heart, left lung, right breast, spinal cord, healthy tissue sparing compared with those using PTV_{0.7} (all $P < 0.01$) (Figures 1, 2 and Table 3).

4 | DISCUSSION

Increasing PTV expansion in post modified radical mastectomy intensity-modulated radiotherapy (PMRM-IMRT) for left-sided breast cancer incredibly leads to the increasing radiation exposure of heart and left lung, which leads to the increasing risk of the long-term radiation injury correspondingly.^{2,5,8,10,11} Considering setup and respiration motion uncertainties, either an isotropic 0.7-cm or an 0.5-cm expanding margin of CTV was referred to as an “approximate value” in published study¹² and should not serve as the golden standard of PTV expansion for all patients. The CTV displacement could differ

significantly among different individuals, among women in different treatment systems, among different phases of a respiratory cycle and among three different dimensional directions within the same patient. Such differences probably cannot be clinically neglected. Moreover, the inter-fractional CTV displacement could be quite different in different treatment systems. More accurately quantifying and minimizing CTV displacement could potentially improve the dose distribution.

In our study, we measured the intra-fractional CTV displacement^{13,14} attributed to respiratory movement by defining nine points on the left chest wall and quantifying their displacement by using the 4D CT. We then measured the inter-fractional CTV displacement resulting from the integrated effect of respiratory movement, thoracic deformation and setup errors by using the on-board cone beam CT. Interestingly, we found that the CTV displacement in post modified radical mastectomy intensity-modulated radiotherapy predominantly arises from inter-fraction rather than from intra-fraction during natural breathing, and differs in three directions either inter-fractionally or intra-fractionally. Tailoring and minimizing PTV expansion three-dimensionally based on inter-fractional CTV displacement

TABLE 3 Dosimetric comparison of PMRM-IMRT for left-sided breast cancer patients using PTV_t with those using PTV_{0.5} or those using PTV_{0.7}.

Parameters	PTV _t	PTV _{0.5}	PTV _{0.7}	p1	p2	p3
PTV						
D _{mean}	51.83 ± 0.19	52.06 ± 0.24	52.43 ± 0.48	0.105	0.018	0.004
D _{2%}	53.58 ± 0.35	54.05 ± 0.42	54.80 ± 0.52	0.001	0.001	0.004
D _{50%}	51.94 ± 0.24	52.20 ± 0.33	52.66 ± 0.58	0.006	0.003	0.002
D _{98%}	49.12 ± 0.18	49.07 ± 0.17	48.63 ± 0.33	0.006	0.005	0.274
V _{95%}	99.57 ± 0.20	99.30 ± 0.55	99.04 ± 0.29	0.160	0.001	0.198
V _{105%}	27.98 ± 9.45	39.47 ± 11.51	53.35 ± 17.41	0.004	0.002	0.003
HI	0.085 ± 0.01	0.095 ± 0.01	0.117 ± 0.01	<0.001	<0.001	0.002
CI	0.513 ± 0.05	0.550 ± 0.04	0.593 ± 0.04	0.001	<0.001	0.001
Heart						
D _{mean}	9.01 ± 2.67	9.84 ± 2.67	11.10 ± 2.97	<0.001	<0.001	<0.001
V _{5Gy}	36.78 ± 5.22	39.58 ± 5.15	43.17 ± 6.73	0.044	0.009	<0.001
V _{10Gy}	25.30 ± 4.26	26.78 ± 4.47	29.76 ± 5.46	0.050	0.023	0.046
V _{20Gy}	13.22 ± 2.53	14.48 ± 2.48	16.74 ± 3.57	0.056	0.021	<0.001
Left lung						
D _{mean}	14.47 ± 1.15	15.45 ± 0.95	16.53 ± 1.22	<0.001	<0.001	<0.001
V _{5Gy}	50.62 ± 1.76	52.78 ± 1.67	54.85 ± 3.26	0.079	0.011	<0.001
V _{10Gy}	39.16 ± 1.95	41.18 ± 1.98	43.31 ± 2.89	0.045	0.006	<0.001
V _{20Gy}	26.72 ± 1.12	28.66 ± 1.05	30.51 ± 2.44	0.067	0.009	<0.001
Right breast						
D _{mean}	3.09 ± 2.24	3.57 ± 2.46	4.12 ± 2.85	0.004	0.004	0.003
Spinal cord						
D _{max}	5.76 ± 2.99	8.12 ± 3.48	9.76 ± 3.23	<0.001	<0.001	0.001
Healthy tissue						
D _{mean}	7.87 ± 1.19	8.48 ± 1.18	9.06 ± 1.19	<0.001	<0.001	<0.001

These data represent statistically significant data ($p < 0.05$), and bold is used to make it more obvious.

Abbreviations: PMRM-IMRT = post modified radical mastectomy intensity-modulated radiotherapy. PTV_t = tailored PTV expansion three-dimensionally. PTV_{0.5} = PTV generated from isotropic 0.5-cm expanding margin of CTV. PTV_{0.7} = PTV generated from isotropic 0.7-cm expanding margin of CTV. Data presented as mean ± standard deviation. D_{mean} = mean dose (Gy). D_{2%} = the maximum dose. D_{98%} = the minimum dose. V_x = volume (%) receiving x dose (Gy) or higher. HI = heterogeneity index. CI = conformity index. P: p values from pair samples t test. p1: PTV_t & PTV_{0.5}, p2: PTV_t & PTV_{0.7}, p3: PTV_{0.5} & PTV_{0.7}.

significantly improves the dosimetry of PMRM-IMRT for left-sided breast cancer patients.

Clinical target volume displacement could be repeatedly quantified intra-fractionally by 4D CT. Inter-fractional CTV displacement could be repeatedly quantified by CBCT. The inter-fractional CTV displacement attributed to the mixed effect of respiratory movement, thoracic deformation and setup errors, measured by on board cone beam CT was much larger than the displacement in the intra-fraction and also differed in three dimensions under natural breathing, with 1.7 ± 1.2 mm in x direction, 2.8 ± 2.3 mm in y direction, and 2.6 ± 2.2 mm in z direction, respectively. Evidently, the PTV expansion of post modified radical mastectomy intensity-modulated radiotherapy (PMRM-IMRT) for left-sided breast cancer patients should be based on the inter-fractional CTV displacement rather than the intra-fractional one during natural breathing. Therefore, we could not obtain respiration-induced CTV displacement-related dosimetric benefit when the real-time respiratory gating technics, one of the most effective approaches to

minimize radiation dose delivery to normal tissue and maximize delivery to tumors under patient's motion caused by respiration,^{15–17} was applied to PMRM-IMRT for left-sided breast cancer patients under natural breathing paradigm.

We expanded CTV 3 mm in x, 4 mm in y, and 4 mm in z direction (the average value of the inter-fractional CTV displacement without correction or optimization) to generate PTV_t and created the corresponding IMRT plans. Our results indicate that PMRM-IMRT plans for left-sided breast cancer patients with PTV_t has dosimetric advantages compared with plans with PTV_{0.5} and those with PTV_{0.7}. given its perfect PTV coverage and better heart and left lung sparing. Additionally, the PMRM-IMRT plans with PTV_{0.5} has dosimetric advantages compared with plans with PTV_{0.7}. owing to their better OARs sparing. Collectively, our data supported that tailoring and minimizing PTV expansion three-dimensionally significantly improves the dosimetry of PMRM-IMRT for left-sided breast cancer patients.

Nevertheless, the average tailored PTV expansion without correction only covered 93.3% of all CTV in x, 63.3% in y, and 66.6% in z direction. To reach better CTV target coverage without increasing the expansion value when applying to clinical practice, we could do a successive of 3D on board cone beam CT verification and position correction inter-fractionally at the first 2 weeks of radiotherapy for each patient, until the inter-fractional CTV displacement was stably and repeatably less than the "tailored PTV expansion" value three-dimensionally. Modality with more individualized tailored or minimized PTV expansion and the availability based on the displacement quantifying of the different parts of the chest wall, as well as the corresponding techniques applied in deep breathing¹⁸ warranted further study.

5 | CONCLUSION

Our study exhibits that the CTV displacement in post modified radical mastectomy intensity-modulated radiotherapy for left-sided breast cancer patients predominantly results from inter-fraction rather than from intra-fraction during natural breathing, and differs in three dimensions either inter-fractionally or intra-fractionally. The respiratory gating technics was not recommended to be applied in PMRM-IMRT for left-sided breast cancer during natural breathing. Tailoring and minimizing PTV expansion three-dimensionally based on inter-fractional CTV displacement can significantly improve the dosimetry of PMRM-IMRT for left-sided breast cancer patients under this respiratory paradigm.

ACKNOWLEDGMENTS

This work was supported by grants from the Natural Science Foundation of Guangdong Province (2018A030307050), the National Natural Science Foundation of China (82071973), and the Medical Scientific Research Foundation of Guangdong Province (No. B2017025). Guangdong Provincial Key Laboratory for Breast Cancer Diagnosis and Treatment (2017B030314116).

ETHICAL DECLARATIONS

The study was performed in accordance with the Declaration of Helsinki, and was approved by the Ethics Committee of the Cancer Hospital of Shantou University Medical College. Informed consent form was obtained from each patient.

AUTHOR CONTRIBUTIONS

Conception and design: Changchun Ma. Financial support: Changchun Ma, Jiyong Zhang. Provision of study materials or patients: Dongsheng Li, Fangcai Wu, Lili Wu, Guoxi Wang. Collection and assembly of data: Jiyong Zhang, Lei Huang, Baotian Huang. Data analysis and interpretation: Changchun Ma, Jiyong Zhang, Lei Huang,

Yan Lin. Manuscript drafting: All authors. Final approval of manuscript: All authors.

CONFLICT OF INTEREST

No conflict of interest.

REFERENCES

1. Ma C, Zhang W, Lu J, et al. Dosimetric comparison and evaluation of three radiotherapy techniques for use after modified radical mastectomy for locally advanced left-sided breast cancer. *Sci Rep*. 2015;5:12274.
2. Darby SC, McGale P, Taylor CW, et al. Long-term mortality from heart disease and lung cancer after radiotherapy for early breast cancer: prospective cohort study of about 300,000 women in US SEER cancer registries. *Lancet Oncol*. 2005;6:557–565.
3. Gagliardi G, Constine LS, Moiseenko V, et al. Radiation dose-volume effects in the heart. *Int J Radiat Oncol Biol Phys*. 2009;76:S77–S85.
4. Prosnitz RG, Hubbs JL, Evans ES, et al. Prospective assessment of radiotherapy-associated cardiac toxicity in breast cancer patients: analysis of data 3 to 6 years after treatment. *Cancer*. 2007;110:1840–1850.
5. Taylor C, Correa C, Duane FK, et al. Estimating the risks of breast cancer radiotherapy: evidence from modern radiation doses to the lungs and heart and from previous randomized trials. *J Clin Oncol*. 2017;35:1641–1649.
6. Wang K, Eblan MJ, Deal AM, et al. Cardiac toxicity after radiotherapy for stage III non-small-cell lung cancer: pooled analysis of dose-escalation trials delivering 70 to 90 Gy. *J Clin Oncol*. 2017;35:1387–1394.
7. van Rijswijk JW, Farag ES, Bouten CVC, et al. Fibrotic aortic valve disease after radiotherapy: an immunohistochemical study in breast cancer and lymphoma patients. *Cardiovasc Pathol*. 2019;45:107176.
8. Darby SC, Ewertz M, McGale P, et al. Risk of ischemic heart disease in women after radiotherapy for breast cancer. *N Engl J Med*. 2013;368:987–998.
9. RTOG Breast Atlas. <https://www.nrgoncology.org/ciro-breast>.
10. Taylor C, McGale P, Brønnum D, et al. Cardiac structure injury after radiotherapy for breast cancer: cross-sectional study with individual patient data. *J Clin Oncol*. 2018;36:2288–2296.
11. McGale P, Darby SC, Hall P, et al. Incidence of heart disease in 35,000 women treated with radiotherapy for breast cancer in Denmark and Sweden. *Radiother Oncol*. 2011;100:167–175.
12. Schubert LK, Gondi V, Sengbusch E, et al. Dosimetric comparison of left-sided whole breast irradiation with 3DCRT, forward-planned IMRT, inverse-planned IMRT, helical tomotherapy, and topotherapy. *Radiother Oncol*. 2011;100:241–246.
13. Reitz D, Carl G, Schönecker S, et al. Real-time intra-fraction motion management in breast cancer radiotherapy: analysis of 2028 treatment sessions. *Radiat Oncol*. 2018;13:128.
14. Ricotti R, Ciardo D, Fattori G, et al. Intra-fraction respiratory motion and baseline drift during breast Helical Tomotherapy. *Radiother Oncol*. 2017;122:79–86.
15. Dasu A, Flejmer AM, Edvardsson A, et al. Normal tissue sparing potential of scanned proton beams with and without respiratory gating for the treatment of internal mammary nodes in breast cancer radiotherapy. *Phys Med*. 2018;52:81–85.
16. Berg M, Lorenzen EL, Jensen I, et al. The potential benefits from respiratory gating for breast cancer patients regarding target coverage and dose to organs at risk when applying strict dose limits to the heart: results from the DBCG HYPO trial. *Acta Oncol*. 2018;57:113–119.

17. Oh SA, Yea JW, Kim SK, et al. Optimal gating window for respiratory-gated radiotherapy with real-time position management and respiration guiding system for liver cancer treatment. *Sci Rep.* 2019;9:4384.
18. Farzaneh MK, Nasser S, Momenzhad M, et al. Design and construction of A laser-based respiratory gating system for implementation of deep inspiration breathe hold technique in radiotherapy clinics. *J Med Signals Sens.* 2018;8:253–262.